Contents

Data report: Middle Miocene to earliest Pleistocene *Trilobatus sacculifer* stable isotopic records, IODP Expedition 371 Site U1506, Tasman Sea[1]

Adriane R. Lam,[2] Jeanette deCuba,[2] Gretl King,[2] and Ravi Kiran Koorapati[2]

[1] Lam, A.R., deCuba, J., King, G., and Koorapati, R.K., 2024. Data report: Middle Miocene to earliest Pleistocene Trilobatus sacculifer stable isotopic records, IODP Expedition 371 Site U1506, Tasman Sea. In Sutherland, R., Dickens, G.R., Blum, P., and the Expedition 371 Scientists, Tasman Frontier Subduction Initiation and Paleogene Climate. Proceedings of the International Ocean Discovery Program, 371: College Station, TX (International Ocean Discovery Program). https://doi.org/10.14379/iodp.proc.371.201.2024

[2] Earth Sciences Department, Binghamton University, USA. Correspondence author: **alam@binghamton.edu**

Abstract

The Late Neogene to Quaternary periods include several climate and tectonic events that brought the surface ocean circulation system into its modern configuration. Characterizing how surface conditions, namely temperature and salinity gradients, behaved in response to cooling and warming events has implications for understanding past atmospheric and biotic processes and how the Earth system may respond to increased anthropogenic warming. One region that lacks long-term geochemical records is the Tasman Sea, southwest Pacific Ocean. This region is characterized by a major western boundary current and its extensional flow, which creates large temperature gradients within the basin. Prior geochemical analyses indicate this region warmed and cooled in response to tectonic gateway closures. To build on these geochemical data sets and create a transect across the northern Tasman Sea, we use $\delta^{18}O$ and $\delta^{13}C$ measurements from the mixed-layer planktic foraminifera species *Trilobatus sacculifer* to reconstruct surface ocean conditions from the Middle Miocene to early Pleistocene (12–2.3 Ma) at International Ocean Discovery Program Site U1506. We find that surface ocean conditions at the site oscillated through time, with some major stepped changes in the isotopic values through the Miocene. Additional geochemical time series developed in the future from more central and southern Tasman Sea sites will aid in understanding the development and behavior of such frontal boundary systems through the Neogene.

1. Introduction

The Late Neogene to Early Quaternary periods (~12–2.3 Ma) are a time of overall global cooling punctuated by climatic shifts and tectonic gateway reconfigurations (Lisiecki and Raymo, 2005; Westerhold et al., 2020). These events include the constriction of the Indonesian Throughflow through the Neogene (reviewed in Kuhnt et al., 2004); the continued and stepwise cooling of southern high latitudes (~14.6–9.0 Ma; Holbourn et al., 2013); the constriction and closure of the Central American Seaway (critical threshold of closure ~4.8–4 Ma; Haug and Tiedemann, 1998; Steph et al., 2010); the mid-Piacenzian Warm Period (3.2–2.9 Ma; e.g., Raymo et al., 1996; Pagani et al., 2010; Martínez-Botí et al., 2015; O'Dea et al., 2016); and the initiation and growth of Northern Hemisphere glaciers (~3.6–2.4 Ma; Mudelsee and Raymo, 2005). These major Earth events led to the surface ocean circulation system and sea surface temperature gradients that characterize today's ocean, especially in the midlatitudes (e.g., Lam et al., 2020, 2021; Sutherland et al., 2022; Singh et al., 2023). Understanding how the surface ocean and temperature gradients responded to such tectonic and climate changes and how they came into their modern configuration has impli-

cations for understanding the ocean systems' influence on atmospheric and biotic processes and how such systems may behave in the future under anthropogenic warming scenarios. The Tasman Sea in the southwest Pacific Ocean, an area dominated by a wide and drastic sea surface temperature gradient, is one region in which we can study the effects of changing climate and tectonic gateway closures on the surface ocean (Figure F1).

The South Pacific Tasman Sea surface ocean circulation system is dominated by the Eastern Australia Current (EAC), the major western boundary current of the South Pacific Gyre system that transports heat and moisture (e.g., Sprintall et al., 1995), and it influences both regional weather (Sprintall et al., 1995) and climate patterns (e.g., Cai et al., 2005). This current flows along the east coast of Australia, where it detaches from the coast between 30° and 34°S and flows eastward. An allotment of the EAC continues southward, around Tasmania (Figure F1). This portion of the current that flows eastward has traditionally been termed the Tasman Front, but recent publications indicate the eastward flow features are only apparent in time-averaged data (Oke et al., 2019a). Instead, where the EAC separates from the Australian coast, there is a complex field of eddies that feed flow from the Australian coast toward New Zealand (Oke et al., 2019a). Oke et al. (2019b) showed the Tasman Front is not a true frontal system and instead suggested calling the area the "EAC southern extension," a term we have adopted here.

Oceanic frontal systems, such as the EAC southern extension, and sea surface temperature gradients in the Tasman Sea developed as a response to the opening of the Drake Passage and growth of Antarctic ice sheets during the Oligocene, leading to the establishment and intensification of the Antarctic Circumpolar Current (Nelson and Cooke, 2001; Pfuhl and McCave, 2005). Despite these findings, few long-term geochemical records have been published from the Tasman Sea to infer how the EAC southern extension responded to tectonic and climate events through the Neogene. Recently, Gastaldello et al. (2023) used stable isotopic analyses and benthic foraminiferal assemblages from International Ocean Discovery Program (IODP) Expedition 371 to characterize the Middle Miocene Biogenic Bloom in the Tasman Sea. They found that the event was complex with multiple phases. Karas et al. (2011) developed a paired $\delta^{18}O$ and Mg/Ca record from the planktonic foraminifera species *Trilobatus sacculifer* for Deep Sea Drilling Program (DSDP) Hole 590B (31.17°S, 163.49°E; Figure F1). Their data indicate the northern Tasman Sea experienced surface
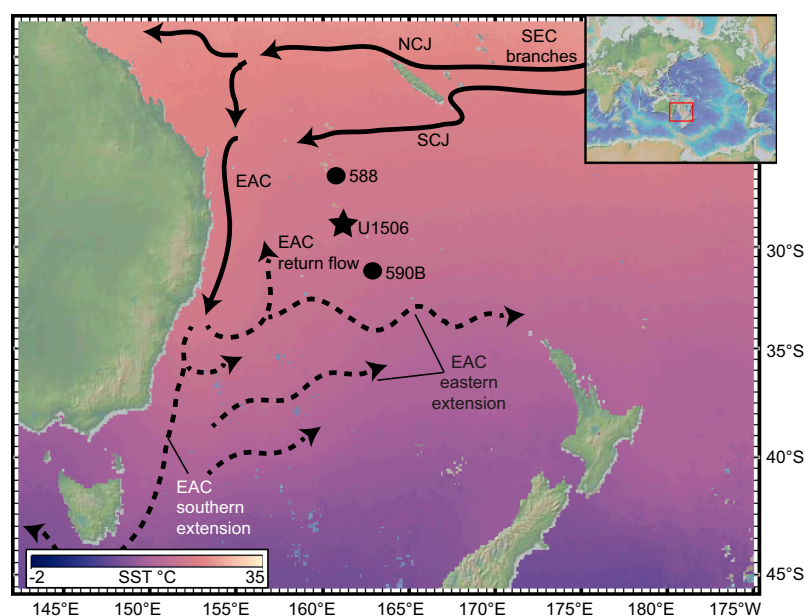
Figure F1. Sea surface temperature and bathymetric map of the Tasman Sea, southwest Pacific Ocean. Black star = location of Site U1506, black circles = DSDP Site 588 and Hole 590B. Solid lines = permanent currents, dashed lines = transient currents and areas of eddy trains. Figure was made using GeoMapApp under a Creative Commons Attribution 4.0 International (CC BY 4.0) license. Inset: location map. SEC = South Equatorial Current, NCJ = North Caledonian Jet, SCJ = South Caledonia Jet. Approximate location of currents and eastward flow fields are from Oke et al. (2019b).

water cooling and freshening in response to the closure of the Central American Seaway. Warming of the northern Tasman Sea after ~3.8 Ma was triggered by a constricting Indonesian Through-flow and intensification of the EAC (Karas et al., 2011). Hodell and Kennett (1986) created a stable isotopic curve for DSDP Site 588 (26.29°S, 161.38°E; Figure **F1**), located north of Hole 590B. Here, there is less variability in the δ¹⁸O signal, but their data also indicate cooling and/or freshening around ~4 Ma associated with the constriction of the Central American Seaway, followed by surface water warming.

To better infer the behavior of the surface ocean conditions through time in the Tasman Sea, we have created a long-term stable isotopic time series ($\delta^{18}O$ and $\delta^{13}C$) at a site located between Site 588 and Hole 590B. We used the mixed-layer planktonic foraminiferal species *T. sacculifer* (Keller and Kennett, 1985) from IODP Site U1506 to construct a record from the Middle Miocene to earliest Pleistocene (~12–2.33 Ma). Our results indicate that at Site U1506, sea surface conditions were variable throughout the study interval, likely as a result of tectonic gateway closures and climate shifts.

2. Materials and methods

A low-resolution (approximately one sample every ~49 ky) mixed-layer stable isotope record was constructed for Site U1506 (28.66°S, 161.74°E; 1494.9 m water depth). For this analysis, 195 10 cm³ bulk sediment samples were dried in an oven at 50°C for approximately 48 h. Bulk samples were weighed and then washed over a 63 µm screen with tap water. Sieved >63 µm residues were then transferred to an oven to dry at 50°C overnight. Once dry, the residues were weighed, vialed, and labeled.

To produce the stable isotopic ($\delta^{18}O$ and $\delta^{13}C$) record for subtropical Site U1506, we picked four to six specimens of *T. sacculifer* (without the elongate sac-like final chamber) from each sample from the 355–425 µm size fraction (see ISOTOPE in **Supplementary material**). We conducted replicates on 12 of the samples used in the study as an a priori test on within-sample variability (Table **T1**). Isotopic results are reported against Vienna Peedee Belemnite (VPDB) using the standard δ notation expressed in permil (‰). Stable isotopic measurements were made on a Finnigan Delta Plus XL ratio mass spectrometer coupled with a GasBench II automated sampler at the University of Massachusetts Amherst. Analytical precision was better than 0.08‰ for $\delta^{18}O$ and 0.06‰ for $\delta^{13}C$ (one standard deviation) based on tracking of uncorrected results for an in-house standard for Site U1506 samples.

Measurements were plotted against depth in the core (Figure **F2**) and on the age model developed using calcareous nannofossil biostratigraphy for Site U1506 (**Sutherland et al.,** 2019), including the tuned age model for part of the section from Gastaldello et al. (2023) (Figure **F3**).

Table T1. Average isotopic value, range, and standard deviation for 12 replicate samples, Site U1506. **Download table in CSV format.**
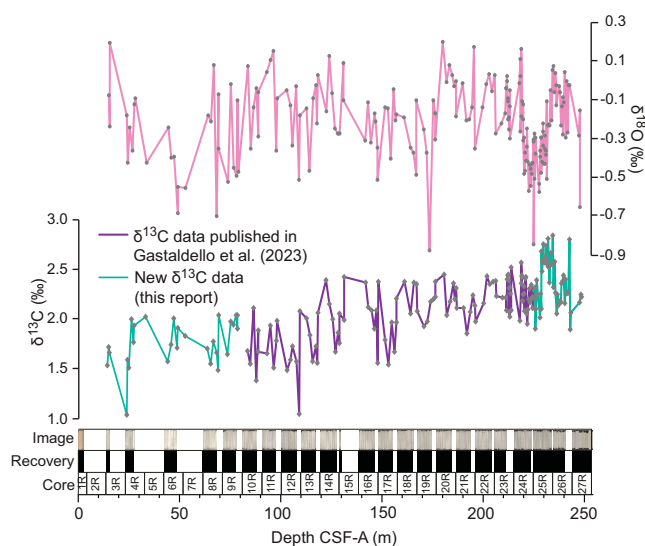
Figure F2. Stable isotopic measurements using *Trilobatus sacculifer* from Site U1506. Core, core recovery, and core images are from Sutherland et al. (2019).
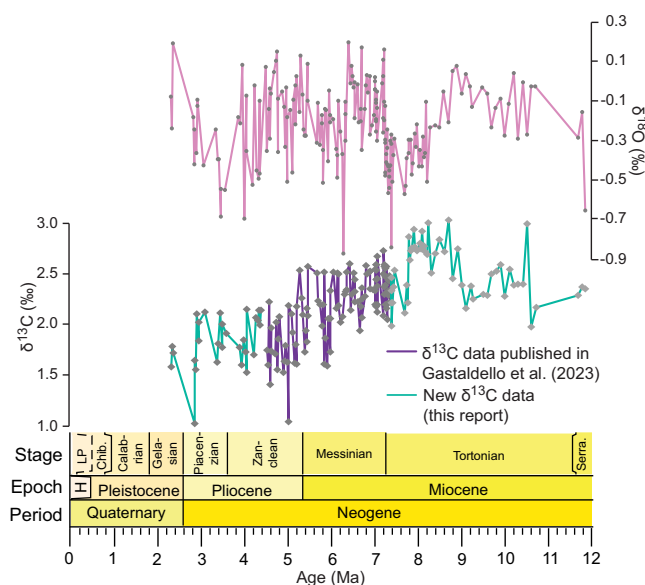
Figure F3. Stable isotopic measurements using *Trilobatus sacculifer* from Site U1506 on the tuned age model of Gastaldello et al. (2023; 4.18–7.41 Ma; 71.80–222.80 m) and the shipboard biostratigraphic age model (Sutherland et al., 2019). LP = Late Pleistocene, Chib. = Chibanian, Serra. = Serravalian, H = Holocene.

3. Results

3.1. Within-sample variability

A total of 12 replicate samples from Site U1506, representing 6% of the total samples, were run to determine within-sample variability (Table **T1**). Intrasample variability (difference within samples) for $\delta^{13}C$ values ranges 0.05‰−0.41‰, and $\delta^{18}O$ sample variability ranges 0.00‰−0.47‰.

3.1.1. Stable isotopic measurements

Throughout the study interval, sea surface temperature and/or salinity changed drastically (Figures **F2**, **F3**). From 12 to ~10.6 Ma, $\delta^{18}O$ values quickly increase, whereas $\delta^{13}C$ values remain

steady around 2.25‰ but exhibit a slight decrease. From ~10.6 to ~8.5 Ma, δ^{18}O values remain largely steady within the range of ~0.3‰–0.1‰. In the same interval, δ^{13}C values exhibit a general decrease, generally around ~2.5‰, with intermittent increases to ~3.0‰ at ~10.5 and 8.8 Ma. The late Tortonian is characterized by decreasing δ^{18}O values, from 0.1‰ at ~8.8 Ma to –0.6‰ at ~7.2 Ma. Carbon isotope values exhibit a decrease from about 2.5‰ at ~8.8 Ma to ~2.0‰ at ~7.2 Ma. The Late Miocene Messinian Stage is characterized by δ^{18}O values that increase and oscillate within the range of about –0.3‰ to 0.1‰ until 6.2 Ma. Within the same time interval (7.2–6.2 Ma), δ^{13}C values oscillate between ~2.5‰ and 2.0‰. The latest Miocene (6.2–5.3 Ma) is characterized by another step decline in the δ^{18}O record, with values decreasing and oscillating between approximately –0.5‰ and –0.1‰ and δ^{13}C values oscillating around 2.5‰–1.6‰.

The stable isotopic records within the Pliocene are generally less variable than the Miocene, with no large and apparent stepwise increases or decreases in stable isotopic values. Generally, the δ^{18}O values from the Early Pliocene to earliest Pleistocene range approximately –0.7‰–0.3‰, and the δ^{13}C values range 2.5‰–1.0‰.

Because these samples are from a midlatitude site, seasonality has likely greatly influenced the stable isotopic values obtained from surface-dwelling planktonic foraminifera (e.g., Lam et al., 2021). Therefore, such abiotic factors should be considered when interpreting geochemical records such as those presented in this data report.

4. Acknowledgments

References

Cai, W., Shi, G., Cowan, T., Bi, D., and Ribbe, J., 2005. The response of the Southern Annular Mode, the East Australian Current, and the southern mid-latitude ocean circulation to global warming. Geophysical Research Letters, 32(23). **https://doi.org/10.1029/2005GL024701**

Gastaldello, M.E., Agnini, C., Westerhold, T., Drury, A.J., Sutherland, R., Drake, M.K., Lam, A.R., Dickens, G.R., Dallanave, E., Burns, S., and Alegret, L., 2023. The Late Miocene-Early Pliocene biogenic bloom: an integrated study in the Tasman Sea. Paleoceanography and Paleoclimatology, 38(4):e2022PA004565. **https://doi.org/10.1029/2022PA004565**

Haug, G.H., and Tiedemann, R., 1998. Effect of the formation of the Isthmus of Panama on Atlantic Ocean thermohaline circulation. Nature, 393(6686):673–676. **https://doi.org/10.1038/31447**

Hodell, D.A., and Kennett, J.P., 1986. Late Miocene–Early Pliocene stratigraphy and paleoceanography of the South Atlantic and southwest Pacific oceans: a synthesis. Paleoceanography, 1(3):285–311. **https://doi.org/10.1029/PA001i003p00285**

Holbourn, A., Kuhnt, W., Clemens, S., Prell, W., and Andersen, N., 2013. Middle to Late Miocene stepwise climate cooling: evidence from a high-resolution deep water isotope curve spanning 8 million years. Paleoceanography, 28(4):688–699. **https://doi.org/10.1002/2013PA002538**

Karas, C., Nürnberg, D., Tiedemann, R., and Garbe-Schönberg, D., 2011. Pliocene climate change of the Southwest Pacific and the impact of ocean gateways. Earth and Planetary Science Letters, 301(1–2):117–124. **https://doi.org/10.1016/j.epsl.2010.10.028**

Keller, G., and Kennett, J.P., 1985. Depth stratification of planktonic foraminifers in the Miocene ocean. In Kennett, J.P., The Miocene Ocean: Paleoceanography and Biogeography. Memoirs - Geological Society of America, 163. **https://doi.org/10.1130/MEM163-p177**

Kuhnt, W., Holbourn, A., Hall, R., Zuvela, M., and Käse, R., 2004. Neogene history of the Indonesian throughflow. In Clift, P., Kuhnt, W., Wang, P., and Hayes, D. (Eds.), Continent-Ocean Interactions Within East Asian Marginal Seas. Geophysical Monograph, 149: 299–320. **https://doi.org/10.1029/149GM16**

Lam, A.R., deCuba, J., King, G., and Koorapati, R.K., 2024. Supplementary material, **https://doi.org/10.14379/iodp.proc.371.201supp.2024**. In Lam, A.R., deCuba, J., King, Gretl, and Koorapati, R.K., Data report: Middle Miocene to earliest Pleistocene Trilobatus sacculifer stable isotopic records, IODP Expedition 371 Site U1506, Tasman Sea. In Sutherland, R., Dickens, G.R., Blum, P., and the Expedition 371 Scientists, Tasman Frontier Subduction Initiation and Paleogene Climate. Proceedings of the International Ocean Discovery Program, 371: College Station, TX (International Ocean Discovery Program).

Lam, A.R., Leckie, R.M., and Patterson, M.O., 2020. Illuminating the past to see the future of western boundary currents: micropaleontological investigations of the Kuroshio Current extension. Oceanography, 33(2):65–67. **https://doi.org/10.5670/oceanog.2020.219**

Lam, A.R., MacLeod, K.G., Schilling, S.H., Leckie, R.M., Fraass, A.J., Patterson, M.O., and Venti, N.L., 2021. Pliocene to Earliest Pleistocene (5–2.5 Ma) reconstruction of the Kuroshio Current extension reveals a dynamic current. Paleoceanography and Paleoclimatology, 36(9):e2021PA004318. **https://doi.org/10.1029/2021PA004318**

Lisiecki, L.E., and Raymo, M.E., 2005. A Pliocene-Pleistocene stack of 57 globally distributed benthic $\delta^{18}O$ records. Paleoceanography, 20(1):PA1003. **https://doi.org/10.1029/2004PA001071**

Martínez-Botí, M.A., Foster, G.L., Chalk, T.B., Rohling, E.J., Sexton, P.F., Lunt, D.J., Pancost, R.D., Badger, M.P.S., and Schmidt, D.N., 2015. Plio-Pleistocene climate sensitivity evaluated using high-resolution CO_2 records. Nature, 518(7537):49–54. **https://doi.org/10.1038/nature14145**

Mudelsee, M., and Raymo, M.E., 2005. Slow dynamics of the Northern Hemisphere glaciation. Paleoceanography and Paleoclimatology, 20(4):PA4022. **https://doi.org/10.1029/2005PA001153**

Nelson, C.S., and Cooke, P.J., 2001. History of oceanic front development in the New Zealand sector of the Southern Ocean during the Cenozoic—a synthesis. New Zealand Journal of Geology and Geophysics, 44(4):535–553. **https://doi.org/10.1080/00288306.2001.9514954**

O'Dea, A., Lessios, H.A., Coates, A.G., Eytan, R.I., Restrepo-Moreno, S.A., Cione, A.L., Collins, L.S., de Queiroz, A., Farris, D.W., Norris, R.D., Stallard, R.F., Woodburne, M.O., Aguilera, O., Aubry, M.-P., Berggren, W.A., Budd, A.F., Cozzuol, M.A., Coppard, S.E., Duque-Caro, H., Finnegan, S., Gasparini, G.M., Grossman, E.L., Johnson, K.G., Keigwin, L.D., Knowlton, N., Leigh, E.G., Leonard-Pingel, J.S., Marko, P.B., Pyenson, N.D., Rachello-Dolmen, P.G., Soibelzon, E., Soibelzon, L., Todd, J.A., Vermeij, G.J., and Jackson, J.B.C., 2016. Formation of the Isthmus of Panama. Science Advances, 2(8):e1600883. **https://doi.org/10.1126/sciadv.1600883**

Oke, P.R., Pilo, G.S., Ridgway, K., Kiss, A., and Rykova, T., 2019a. A search for the Tasman Front. Journal of Marine Systems, 199:103217. **https://doi.org/10.1016/j.jmarsys.2019.103217**

Oke, P.R., Roughan, M., Cetina-Heredia, P., Pilo, G.S., Ridgway, K.R., Rykova, T., Archer, M.R., Coleman, R.C., Kerry, C.G., Rocha, C., Schaeffer, A., and Vitarelli, E., 2019b. Revisiting the circulation of the East Australian Current: its path, separation, and eddy field. Progress in Oceanography, 176:102139. **https://doi.org/10.1016/j.pocean.2019.102139**

Pagani, M., Liu, Z., LaRiviere, J., and Ravelo, A.C., 2010. High Earth-system climate sensitivity determined from Pliocene carbon dioxide concentrations. Nature Geoscience, 3(1):27–30. **https://doi.org/10.1038/ngeo724**

Pfuhl, H.A., and McCave, I.N., 2005. Evidence for late Oligocene establishment of the Antarctic Circumpolar Current. Earth and Planetary Science Letters, 235(3–4):715–728. **https://doi.org/10.1016/j.epsl.2005.04.025**

Raymo, M.E., Grant, B., Horowitz, M., and Rau, G.H., 1996. Mid-Pliocene warmth: stronger greenhouse and stronger conveyor. Marine Micropaleontology, 27(1–4):313–326. **https://doi.org/10.1016/0377-8398(95)00048-8**

Singh, V.P., Pathak, S., and Dwivedi, R., 2023. Reduction in the strength of Agulhas Current during Quaternary: planktic foraminiferal records for 1.2 million years from IODP Hole U-1474A. Journal of Climate Change, 9:45–52. **https://doi.org/10.3233/JCC230031**

Sprintall, J., Roemmich, D., Stanton, B., and Bailey, R., 1995. Regional climate variability and ocean heat transport in the southwest Pacific Ocean. Journal of Geophysical Research: Oceans, 100(C8):15865–15871. **https://doi.org/10.1029/95JC01664**

Steph, S., Tiedemann, R., Prange, M., Groeneveld, J., Schulz, M., Timmermann, A., Nürnberg, D., Rühlemann, C., Saukel, C., and Haug, G.H., 2010. Early Pliocene increase in thermohaline overturning: a precondition for the development of the modern equatorial Pacific cold tongue. Paleoceanography, 25(2):PA2202. **https://doi.org/10.1029/2008PA001645**

Sutherland, R., Dickens, G.R., Blum, P., Agnini, C., Alegret, L., Asatryan, G., Bhattacharya, J., Bordenave, A., Chang, L., Collot, J., Cramwinckel, M.J., Dallanave, E., Drake, M.K., Etienne, S.J.G., Giorgioni, M., Gurnis, M., Harper, D.T., Huang, H.-H.M., Keller, A.L., Lam, A.R., Li, H., Matsui, H., Morgans, H.E.G., Newsam, C., Park, Y.-H., Pascher, K.M., Pekar, S.F., Penman, D.E., Saito, S., Stratford, W.R., Westerhold, T., and Zhou, X., 2019. Site U1506. In Sutherland, R., Dickens, G.R., Blum, P., and the Expedition 371 Scientists, Tasman Frontier Subduction Initiation and Paleogene Climate. Proceedings of the International Ocean Discovery Program, 371: College Station, TX (International Ocean Discovery Program). **https://doi.org/10.14379/iodp.proc.371.103.2019**

Sutherland, R., Santos, Z.D., Agnini, C., Alegret, L., Lam, A.R., Westerhold, T., Drake, M.K., Harper, D.T., Dallanave, E., Newsam, C., Cramwinkel, M.J., Dickens, G.R., Collot, J., Etienne, S.J.G., Bordenave, A., Stratford, W.R., Zhou, X., Li, H., and Asatryan, G., 2022. Neogene mass accumulation rate of carbonate sediment across northern Zealandia, Tasman Sea, southwest Pacific. Paleoceanography and Paleoclimatology, 37(2):e2021PA004294. **https://doi.org/10.1029/2021PA004294**

Westerhold, T., Marwan, N., Drury, A.J., Liebrand, D., Agnini, C., Anagnostou, E., Barnet, J.S.K., Bohaty, S.M., De Vleeschouwer, D., Florindo, F., Frederichs, T., Hodell, D.A., Holbourn, A.E., Kroon, D., Lauretano, V., Littler, K., Lourens, L.J., Lyle, M., Pälike, H., Röhl, U., Tian, J., Wilkens, R.H., Wilson, P.A., and Zachos, J.C., 2020. An astronomically dated record of Earth's climate and its predictability over the last 66 million years. Science, 369(6509):1383–1387. **https://doi.org/10.1126/science.aba6853**